

## **Electromechanical modelling and experimental analysis of a compression-based piezoelectric vibration energy harvester**

X.Z Jiang<sup>1</sup>, Y.C Li<sup>1\*</sup>, J. Wang<sup>2</sup>, and J.C Li<sup>1</sup>

*<sup>1</sup>Centre for Built Infrastructure Research, Faculty of Engineering and Information Technology, University of Technology Sydney, PO Box 123, 15 Broadway, NSW 2007, Australia*

*<sup>2</sup>School of Mechanical Engineering, Nanjing University of Science & Technology, 200 Xiaolingwei Street, Xuanwu District, Nanjing 210094, China*

\*Corresponding author: Dr. Yancheng Li

Correspondence: City Campus, Bldg 1 Lvl 24 Rm 17C, PO Box 123 Broadway, NSW 2007, Australia

T: +61 2 9514 2403

F: +61 2 9514 2435

Email: [yancheng.li@uts.edu.au](mailto:yancheng.li@uts.edu.au)

# **Electromechanical modelling and experimental analysis of a compression-based piezoelectric vibration energy harvester**

Over the past few decades, wireless sensor networks have been widely used in the field of structure health monitoring of civil, mechanical and aerospace systems. Currently, most wireless sensor networks are battery-powered and it is costly and unsustainable for maintenance because of the requirement for frequent battery replacements. As an attempt to address such issue, this paper theoretically and experimentally studies a compression-based piezoelectric energy harvester using a multilayer stack configuration, which is suitable for civil infrastructure system applications where large compressive loads occur, such as heavily vehicular loading acting on pavements. In this paper, we firstly present analytical and numerical modelling of the piezoelectric multilayer stack under axial compressive loading, which is based on the linear theory of piezoelectricity. A two-degree-of-freedom (2DOF) electromechanical model, considering both the mechanical and electrical aspects of the proposed harvester, was developed to characterize the harvested electrical power under the external electrical load. Exact closed-form expressions of the electromechanical models have been derived to analyze the mechanical and electrical properties of the proposed harvester. The theoretical analyses are validated through several experiments for a test prototype under harmonic excitations. The test results exhibit very good agreement with the analytical analyses and numerical simulations for a range of resistive loads and input excitation levels.

Keywords: Vibration Energy Harvesting; Piezoelectric; 2DOF Electromechanical Model; Large-force; Low-frequency

## **1. Introduction**

Because of the advantages over existing wired technologies, wireless sensors and sensor networks have become ubiquitous in the field of civil structure health monitoring in recent years. Currently, the wireless sensors network is battery-powered and it is not only costly for maintenance but the requirement for frequent battery replacements raises serious reliability and sustainability issues in practice. The task of replacing battery

sometimes can become extremely difficult, especially in case of structural health monitoring applications, where there are hundreds and thousands of sensors that are often installed during construction stages. For these sensors, if it is not impossible, for the least it is impractical to gain access, remove protection and replace batteries. The disposal of large quantities of batteries may also lead to serious environmental hazards.

Although the power requirement of a single wireless node is quite low (normal lower than hundreds of  $\mu\text{W}$ ), the wireless sensor network required significant power supply since the number of the sensor nodes and the computational demands have drastically increased due to advanced algorithms to enable performance of structural health monitoring [1], especially for large-scale civil infrastructures. So it is of great necessity to seek alternative power sources for the sensor networks. Due to the low-power consumption requirements of an individual wireless sensor, a possible solution to this problem is the technologies that enable harvesting ambient vibration mechanical energy to power wireless sensor networks [1,2].

Obtaining power from ambient vibration sources is generally known as vibration energy harvesting, or vibration energy scavenging. Several methods, such as electromagnetic induction, electrostatic generation, and piezoelectric generation, can be utilized to harvest electrical energy from external vibrations [3]. While each of the aforementioned methods can generate a useful amount of energy, piezoelectric materials have received more attentions especially in the recent years due to their ability to directly convert applied strain energy into usable electrical energy, as well as its large power density, and ease of application [4-6]. Comparing to energy harvesting for large-scale alternative energy generation using wind turbines and solar cells is mature technology, the development of energy harvesting technology by using piezoelectric devices on a scale appropriate for small, low-power, embedded wireless sensing

**Formatted:** Font: Italic, English (U.S.)

systems is still in its developmental stage, particularly for application of structural health monitoring sensing system. In 2002, Elvin et al. proposed a self-powered damage detection sensor using piezoelectric patches [7]. A piezoelectric harvester in cantilever beam configuration is utilized to convert the applied load into electricity and provide a power for the sensors in order to measure the strain and to send the results to a moving cart. In 2006, Discenzo et al. developed a prototype self-powered sensor node that performs sensing, local processing, and telemeters the results to a central node for pump condition monitoring applications [8]. The device was mounted on an oil pump, and a cantilever piezoelectric beam tuned to the excitation frequency was embedded with the sensor node to scavenge energy from the pump vibration. The test results showed that the output power could reach to 40mW. In 2008, Lallart et al. proposed a self-powered wireless structural health monitoring system [9]. A piezoelectric harvester based on the beam structure, using the synchronized switch harvesting method, was utilized to convert ambient mechanical energy into electricity and powered the structure health monitoring system. In 2011, Kim et al. investigated the possibility of harvesting energy from bridges by converting the potential energy of vibrating bridge systems into electrical energy using a cantilever piezoelectric harvester, and got some good results [10]. Of the published results that focus on using piezoelectric harvesters scavenging electricity for the wireless sensor networks, most of them have focused on harvesting energy using cantilever beams configuration [11-13]. However, the cantilever beam cannot sustain large force, and in large force vibration environments, such as the large compressive loadings induced by the heavy trucks on the pavement, the piezoelectric harvester in cantilever beam configuration would be more frangible and breakable.

In this paper, a compression-based piezoelectric harvester was developed to scavenge energy from surrounding vibrations in order to provide power for the wireless

sensor networks. The piezoelectric material used in this novel harvester is constructed in multilayer stack configuration that is robust and suitable for large force vibrations existing in the civil infrastructure system applications. In comparison with the monolithic configuration, the stack structure can reduce the voltage output and the matching resistive load of the harvester to a more manageable level [14], therefore the piezoelectric stack is selected in this research to scavenge vibration energy. By now, the development of models for cantilevered piezoelectric harvester has attracted a great deal of attentions from researchers. And there are already many models available to evaluate the harvested power of cantilevered harvester [15-17]. [Roundy et al. \[18\]](#), [Aldraihem and Baz \[19\]](#) have ~~done~~conducted some studies on the multiple-DOF models of cantilevered piezoelectric harvesters. [Tang and Yang \[20\]](#) presented a novel multiple-DOF harvesting model of the cantilevered piezoelectric harvester. [Wu et al. \[21\]](#) presented a nonlinear 2-DOF model of the cantilevered piezoelectric harvester to [enhance the performance of piezoelectric energy harvesters](#). However, to date, there is limited research reported on the development of stack configuration based piezoelectric harvesters. [Keawboonchuay and Engel \[1822,1923\]](#), [Platt et al. \[14, 2024\]](#), [Feenstra et al. \[2125\]](#) have done some feasibility investigations on the piezoelectric harvester in stack configuration, however comprehensive research on the piezoelectric harvester constructing in multilayer stack configuration is still limited. Moreover, a piezoelectric harvester system contains two fundamental elements: the mechanical part that generates electrical energy, and an electrical circuit that converts and rectifies the generated energy in a form of an alternating voltage, into a constant voltage. The efficiency of the energy harvester design depends not only on the piezoelectric harvester itself but also on its integration with the electrical circuit. Therefore, an electromechanical model which considers both the mechanical and electrical aspects of the proposed harvester is

of great importance to optimize the design as well as for understanding the behavior of the piezoelectric harvester.

In this paper, we will firstly investigate the longitudinal mode of the piezoelectric stack for the aim of finding the inter-medium force that will be used to convert vibration energy into electrical energy. Then, the electromechanical model of the proposed compression-based piezoelectric stack harvester will be presented to investigate the ability of harvesting electrical power and analyse the electrical properties of the harvester. Finally, we will present a series of tests conducted to verify the theoretical findings. Test results strongly verify the validity of the proposed theoretical analysis and show that the harvester can generate a maximum 200 mW electrical power under the harmonic excitation with 1360 N amplitude and 6 Hz frequency. Also, the harvested electrical power is proportional to the level of external excitation.

## **2. Electromechanical models**

### ***2.1 Electrical characteristics of the piezoelectric wafer-stack***

The vibration energy harvester proposed in this paper employs piezoelectric multilayer stack in order to endure large compressive loads that exist in the field of civil infrastructure systems application. In practice, the proposed harvester can be embedded into the civil building, roads and highways to harvest electrical energy, just like the energy harvesting system shown in INNOWATTECH LTD.'s patent [26]. When subjected to an external force, the piezoelectric stack will produce an electric charge and convert external kinetic energy into electricity. Therefore, the piezoelectric stack is the media to convert kinetic energy to electrical energy and it is necessary to investigate the electrical reaction of the stack under external excitation before developing an accurate model to present a piezoelectric harvester. Figure 1 shows the sketch of the

piezoelectric stack under applying external force. The force,  $F(t)$ , used in this analysis is a harmonic excitation in order to simplify the analysis. The rubber, as shown in Figure 1, is used to protect the wafer-stack from damage under external large force due to the brittleness of piezoelectric materials.

According to the IEEE Standard on Piezoelectricity: under the external force, giving by the strain  $S$ , stress  $T$ , electric field  $E$ , and electric displacement  $D$ , the constitutive relations of the piezoelectric energy harvesting device are typically defined by:

$$\begin{bmatrix} T_3 \\ D_3 \end{bmatrix} = \begin{bmatrix} c_3^E & -e_{33} \\ e_{33} & \varepsilon_{33}^s \end{bmatrix} \begin{bmatrix} S_3 \\ E_3 \end{bmatrix} \quad (1)$$

where the  $e_{33}$  is the piezoelectric coefficient,  $c_3^E$  is the elastic stiffness constant under a constant electric field, and  $\varepsilon_{33}^s$  is the dielectric constant under constant strain. Note that the subscripts of the state variables show that all constitutive qualities are generated and applied on the thickness direction of the piezoelectric material.

Figure 2 shows the electrical characteristics of the piezoelectric stack, and it needs to point out that the polarization direction of each wafer is opposite to each other. For the configuration as shown in Figure 2, the constitutive equations of the piezoelectric wafer-stack can be written as:

$$S_3 = x_p/h, \quad E_3 = V_p/h, \quad T_3 = F/A, \quad D_3 = Q/A \quad (2)$$

where  $x_p$  is the strain of the piezoelectric wafer-stack under the external force;  $V_p$  is the output voltage of the wafer-stack;  $Q$  is the electric charge;  $A$  is the cross-section area of the wafer-stack, and  $h$  is the length of the wafer-stack. To simplify the analysis, we assume the length of the stack is equal to the entire thickness of all the piezoelectric wafers ( $h=nt$ ) with identical dimension, where  $n$  and  $t$  are the number and thickness of a

single piezoelectric wafer, respectively. According to the relationship in Equation (2), the constitutive equations of the piezoelectric wafer-stack from Equation (1) can be rewritten as:

$$\begin{bmatrix} F \\ Q \end{bmatrix} = \begin{bmatrix} k_p & -N \\ N & C_p \end{bmatrix} \begin{bmatrix} x_p \\ V_p \end{bmatrix} \quad (3)$$

It can be found from Equation (3) that the  $V_p$  is generated by the external force. The force applied to the piezoelectric disc without any electrical input can produce deformation  $x_p$ , the relationship of which is regarded as the elastic coefficient  $k_p$  of the mechanical characteristic. Piezoelectricity also possesses an electrical property between the voltage and the electric charge, which can be modeled as a capacitor  $C_p$ . The electromechanical conversion coefficient  $N$  is defined as the electromechanical coupling coefficient. Based on Equation (3), there is a critical force which is actually used to generate electrical voltage. This critical force can be denoted as  $F_e$  and written as:

$$F_e = NV_p \quad (4)$$

Equation (4) gives an explicit relationship of vibration force and output voltage, which will be used to build the electromechanical model of the piezoelectric harvester.

## **2.2 2DOF electromechanical model without a rectifier circuit**

Considering the mechanical and electrical characteristics of the rubber and piezoelectric stack under the external force, the electromechanical model without a rectified circuit of the proposed harvester is illustrated in Figure 3. As shown in Figure 3,  $F(t)$  is the excitation force. Parameters,  $m_r$ ,  $c_r$ , and  $k_r$ , are used to represent the mass, damping and elastic coefficient of the rubber layer, respectively. Parameters,  $m_p$  and  $k_p$ , are used to represent the mass and elastic coefficients of the piezoelectric wafer-stack, respectively.

Formatted: Font: Italic



Parameters,  $c_h$  and  $k_h$ , are used to represent the mechanical damping and elastic coefficients of the mechanical structure of the harvester, respectively. Parameters,  $x_r$  and  $x_p$ , are used to represent the deformation of the rubber layer and piezoelectric wafer-stack under the external force, respectively. Parameter,  $C_p$ , is used to represent the clamped capacitance of the piezoelectric wafer-stack, and  $R_p$  is the piezoelectric leakage resistance and used to represent the electric loss property of the piezoelectric wafer-stack.  $R_l$  is used to represent the external electrical load.  $I$  and  $V_p$  are used to represent the output current and voltage of the harvester.  $F_e$  is used to link the mechanical parts and electrical parts of the model and convert mechanical energy into electrical energy.

The governing equations of the model can be written as:

$$\begin{cases} m_r \ddot{y} + c_r \dot{y} + k_r y = F(t) - m_r \ddot{x}_p \\ m_p \ddot{x}_p + c_h \dot{x}_p + k_h x_p + k_p x_p + F_e = F(t) - m_r \ddot{x}_p - m_r \dot{y} \\ -N \dot{x}_p + C_p \dot{V}_p + \frac{V_p}{R} = 0 \end{cases} \quad (5)$$

where  $y$  is defined as  $y = x_r - x_p$ ;  ~~$x_r$  and  $x_p$  are the deformation of the rubber and piezoelectric wafer stack under the external force, respectively;~~  $m_r$ ,  $c_r$  and  $k_r$  are the mass, damping and elastic coefficient of the rubber, respectively;  ~~$m_p$  and  $k_p$  are the mass and elastic coefficients of the piezoelectric wafer stack, respectively;~~  $c_h$  and  $k_h$  are the mechanical damping and elastic coefficients of the harvester, respectively;  $\frac{V_p}{R}$ , i.e.  $I$ , is

the current output of the harvester;  ~~$C_p$  is the clamped capacitance of the piezoelectric wafer stack;~~  $R_p$  is the piezoelectric leakage resistance and used to represent the electric loss property of the piezoelectric wafer stack;  ~~$R_l$  is the external electrical load;~~  $R$  is the equivalent resistance of two parallel resistances  $R_p$  and  $R_l$ . In general, the  $R_p$  is much higher than the load resistance, so that  $R \approx R_l$ .

Formatted: Font: Italic

Formatted: Font: Italic

Formatted: Subscript

Field Code Changed

Transforming Equation (5) into the frequency domain and dividing the first equation by  $m_r$ , the second equation by  $m_p$  and the third equation by  $C_p$ , obtain:

$$\begin{cases} (-\omega^2 + 2\zeta_1\omega_1\omega j + \omega_1^2)Y(\omega) - \omega^2 X_p(\omega) = \frac{F(\omega)}{m_r} \\ [-(1+\mu)\omega^2 + 2\zeta_2\omega_2\omega j + \omega_2^2]X_p(\omega) - \mu\omega^2 Y(\omega) + \frac{NV_p(\omega)}{m_p} = \frac{F(\omega)}{m_p} \\ -\frac{\omega NjX_p(\omega)}{C_p} + (\omega j + \frac{1}{RC_p})V_p(\omega) = 0 \end{cases} \quad (6)$$

Here  $\omega$  is the angular frequency of the exciting vibration;  $Y_p(\omega)$ ,  $X_p(\omega)$ ,  $V_p(\omega)$  and  $F(\omega)$  are the frequency counterparts of  $y$ ,  $x_p$ ,  $V_p$  and  $F(t)$ . Other parameters, i.e.  $\omega_1$ ,  $\omega_2$ ,  $\zeta_1$ ,  $\zeta_2$ ,  $\mu$ , are defined as:

$$\omega_1 = \sqrt{\frac{k_r}{m_r}}, \quad \omega_2 = \sqrt{\frac{k_a}{m_p}}, \quad \zeta_1 = \frac{c_r}{2\sqrt{m_r k_r}}, \quad \zeta_2 = \frac{c_h}{2\sqrt{m_p k_a}}, \quad \mu = \frac{m_r}{m_p}, \quad k_a = k_p + k_h \quad (7)$$

Solving Equation (6), obtain:

$$X_p(\omega) = \frac{\frac{(\alpha^2 + 2\zeta_1\psi\alpha j)F(\omega)}{k_a(\alpha^2 - \psi^2 + 2\zeta_1\psi\alpha j)}}{1 - (1+\mu)\psi^2 + 2\zeta_2\psi j - \frac{\mu\psi^4}{\alpha^2 - \psi^2 + 2\zeta_1\psi\alpha j} + \frac{\beta\psi k_e^2 j}{1 + \beta\psi j}} \quad (8)$$

$$V_p(\omega) = \frac{\frac{(\alpha^2 + 2\zeta_1\psi\alpha j)F(\omega)}{N(\alpha^2 - \psi^2 + 2\zeta_1\psi\alpha j)}}{\left[1 - (1+\mu)\psi^2 + 2\zeta_2\psi j - \frac{\mu\psi^4}{\alpha^2 - \psi^2 + 2\zeta_1\psi\alpha j}\right] \frac{1 + \beta\psi j}{\beta\psi k_e^2 j} + 1} \quad (9)$$

where  $\alpha$  and  $\psi$  are the normalized frequencies;  $\beta$  is the normalized electrical resistance;  $k_e$  is the alternative electromechanical coupling coefficient. Those dimensionless parameters can be calculated as:

$$\alpha = \frac{\omega_1}{\omega_2}, \quad \psi = \frac{\omega}{\omega_2}, \quad \beta = \omega_2 RC_p, \quad k_e^2 = \frac{N^2}{C_p k_a} \quad (10)$$

Based on Equation (9), the voltage generated by the harvester can be rewritten as:

$$V_p(\omega) = \frac{F(\omega)k_e^2\beta\psi\alpha}{N(A_3^2 + A_4^2)} [(A_3\alpha + 2A_4\zeta_1\psi) + (2A_3\zeta_1\psi - A_4\alpha)j] \quad (11)$$

where parameters  $A_3$  and  $A_4$  can be calculated as:

$$\begin{cases} A_3 = A_1\beta\psi + (\alpha^2 - \psi^2)\beta k_e^2\psi + A_2 \\ A_4 = A_2\beta\psi + 2\zeta_1\alpha\beta k_e^2\psi^2 - A_1 \end{cases} \quad (12)$$

In Equation (12), parameters  $A_1$  and  $A_2$  are defined as:

$$\begin{cases} A_1 = \alpha^2 - \psi^2 - (1 + \mu)\alpha^2\psi^2 + \psi^4 - 4\zeta_1\zeta_2\psi^2\alpha \\ A_2 = 2\psi [\alpha(1 - \psi^2 - \mu\psi^2)\zeta_1 + (\alpha^2 - \psi^2)\zeta_2] \end{cases} \quad (13)$$

Therefore, based on Equation (11), the electrical power generated by the harvester can be calculated as:

$$P = \frac{V_p \times V_p^*}{2R} = \frac{F(\omega)^2 k_e^4 \beta^2 \psi^2 \alpha^2 [(A_3\alpha + 2A_4\zeta_1\psi)^2 + (2A_3\zeta_1\psi - A_4\alpha)^2]}{2N^2(A_3^2 + A_4^2)^2 R} \quad (14)$$

In Equation (14),  $V_p^*$  is the complex conjugate of  $V_p$ . From the Equation (14), it can be concluded that the electrical power, generated by the presented piezoelectric stack harvester, depends on the external vibration characteristics (frequency  $\psi$  and amplitude  $F(\omega)$ ), the mechanical coefficients-properties of the system (such as the natural frequency  $\omega_1$  and  $\omega_2$ , the mechanical damping factor  $\zeta_1$  and  $\zeta_2$ , and the stiffness of the harvester  $k_a$ ), and the electrical properties of the harvesting system (such as the

Formatted: Font: Italic

Formatted: Subscript

Formatted: Font: Italic

Formatted: Subscript

Formatted: Font: Italic

Formatted: Subscript

Formatted: Font: Italic

Formatted: Subscript

normalized electrical load  $\beta$ , and the overall electromechanical coupling coefficient of the harvester  $k_e$ ). Also, the value of parameters  $A_3$ ,  $A_4$  and  $\beta$  are all dependent on the electrical load  $R$ , therefore the value of the load has a great impact on the electrical power output of the harvester. It is of great need to find out the optimal external resistive load, on which the power generated by the harvester reaches its maximum value.

Based on the Equation (14), the optimal resistive load and the maximum electrical power generated by the harvester can be calculated as:

$$R_{opt} = \frac{A}{(A + \alpha^2 k_e^2 - \psi^2 k_e^2) C_p \omega} \quad \text{and} \quad P_{max} = \frac{F(\omega)^2 \alpha^4 k_e^4 C_p \omega}{4N^2 A (A + \alpha^2 k_e^2 - \psi^2 k_e^2)} \quad (15)$$

where  $A = \alpha^2 - \psi^2 - (1 + \mu)\alpha^2 \psi^2 + \psi^4$

Normally, the nature frequency of the piezoelectric stack is very high (around 1.78e4 Hz in this design). Therefore, based on Equation (10), it is reasonable to assume that the normalized frequency  $\psi$  can be set to zero under low input frequency conditions (lower than 10 Hz). Under this assumption, the optimal electrical load and the maximum generated power can be rewritten as:

$$R_{opt} = \frac{1}{(1 + k_e^2) C_p \omega} \quad \text{and} \quad P_{max} = \frac{F(\omega)^2 k_e^2 \omega}{4k_a (1 + k_e^2)} \quad (16)$$

Equation (16) indicates that the maximum electrical power generated by the proposed piezoelectric harvester is proportional to the frequency of external excitation. And the maximum harvested energy is proportional to the square of the force amplitude of external excitation. Therefore, it indicates that the proposed compression-based piezoelectric vibration harvester is a linear system, the output power of the harvester increases with the input excitation level. It can also be found that the

generated electrical power increases with the electromechanical coupling coefficient  $k_e$ . Equation (10) shows that the value of  $k_e$  is determined by the mechanical framework of the harvester and the properties of the selected piezoelectric materials. Therefore, careful selection of the piezoelectric material and optimal design of the mechanical structure are very important to obtain higher electromechanical coupling coefficient  $k_e$  resulting in optimal scavenging electrical energy under ambient vibration.

Meanwhile, Equation (16) shows that the optimal external resistive load for the maximum electrical power generation is not a constant value and changes with the parameters of the harvester, the properties of the piezoelectric material and the input frequency. The value of the optimal resistive load is inversely proportional to the input frequency and the capacitance of the piezoelectric material. For a weak electromechanical coupling coefficient  $k_e$ , the optimal electrical load can be simplified as  $1/C_p\omega$ .

### **3. Experimental testing**

#### ***3.1 Experimental setup***

The proposed piezoelectric harvester was designed and fabricated to verify the theoretical findings. The sketch of the test setup is shown in Figure 4, and Figure 5 gives the photo of the test system. As shown in Figure 4, the piezoelectric stacks are installed in a host-structure to form the harvester system. Table 1 gives the properties of the piezoelectric stack. Three stacks connected in parallel are used in this design to scavenge electrical energy. One side of the host-structure is fixed on the ground and another side is connected to the shake table which is used to input the vibration excitations. An outer-spring, as shown in Figure 4, was used to transfer shake table's motions into vibrational force and apply on the harvester. The stiffness of the outer-

spring has been tested and shown in Figure 6, and the spring stiffness is 34 N/mm. In the test, the shake table firstly compressed the outer-spring for 50mm as pre-load (i.e. 1700 N) on the piezoelectric harvester, and then reset to zero. Afterward, the shake table performs different harmonic motions with different amplitudes (i.e. 10 mm, 20 mm, 30 mm and 40 mm) and applies exciting harmonic mechanical loads with different amplitudes (i.e. 340 N, 680 N, 1020 N, and 1360 N) on the test prototype by using the outer-spring. The harvester generates electrical power when the exciting loads from the shake table apply on the piezoelectric stacks. Two series-connected rheostats, as shown in Figure 5, were chosen to serve as the electrical load of the harvester in order to investigate the relationship between the power output and the electrical resistance. Data acquisition system was used to record the output voltage signal applied on the electrical load.

### ***3.2 Experimental results comparison and discussion***

Figure 7 shows the actual exciting force applied on the piezoelectric harvester and the real-time output voltage of the harvester with 750 k $\Omega$  electrical load when the shake table performs 20mm/2Hz sinusoidal motion. It can be seen that the preloading force is 1700 N and the harmonic force applied on the harvester has 680 N amplitude and 2 Hz frequency when the shake table performs 20mm/2Hz sinusoidal motion. Under this harmonic force, the voltage generated by the piezoelectric harvester is an AC voltage with the same frequency of the external excitation. Also, as shown in Figure 7, there is a phase change between the excitation and the output voltage, which is caused by the response time of the outer-spring and energy harvesting system itself.

Under the same input shown in Figure 7, Figure 8 shows the real-time output voltages of the proposed piezoelectric stack harvester on different electrical loads, i.e. 292 k $\Omega$ , 480 k $\Omega$  and 750 k $\Omega$ . It can be seen that the voltage output of the harvester is an

AC voltage and its amplitude increases with the external resistance. Figure 8 indicates that the output voltage of the proposed piezoelectric stack harvester under vibrational excitation relates to external electrical loads.

Figure 9 and Figure 10 give the relationships between the amplitudes of the generated voltage/power with different external electrical loads under the applied excitation shown in Figure 7, i.e. 680N/2Hz excitation. Figure 9 indicates that the amplitude of the output voltage, within a certain range of external resistance, increases with the value of the external loads, and then trend to constant after the external resistance exceeding a certain value. And Figure 10 indicates that the power generated by the proposed harvester firstly increases with the value of external loads, and then trends to decrease after the external resistance exceeding a certain value. Based on the results of Figure 9 and Figure 10, it can be obtained that the electrical power generated by the compression-based piezoelectric harvester depends not only on the harvester itself but also on the external electrical load, and there is an optimal electrical load, on which the electrical power harvested by the harvester reaches maximum value under given exciting vibration environment.

Figure 11 and Figure 12 show the relationship between the output voltage/power and the external loads under the excitations with different force amplitudes, i.e. 340 N, 680 N, 1020 N and 1360 N, and fixed frequency, 2 Hz. It can be obtained that: (1) the electrical power generated by the harvester increases with the amplitudes of exciting forces, and the maximum harvested power increases, from 2mW to 45mW, when the exciting force amplitude increases from 340 N to 1360 N; (2) the optimal electrical load does not change its value with the exciting force amplitude under the fixed frequency.

Figure 13 and Figure 14 show the relationship between the output voltage/power and the external loads under the excitations with different frequency, i.e. 1 Hz, 2 Hz, 4

Hz and 6 Hz, and fixed force amplitude, 1360 N. It can be obtained that: (1) the electrical power generated by the harvester increases with the frequency of external excitation, and the maximum harvested power increases from 25 mW to 200 mW, when the exciting frequency increases from 1 Hz to 6 Hz; (2) the value of the optimal electrical load is inversely proportional to the input frequency of the excitation, and its value decreases from 1400 k $\Omega$  to 300 k $\Omega$ , when the exciting frequency increases from 1 Hz to 6 Hz.

For the aim of clearly showing the relationship between the harvested electrical energy with the external excitation, Figure 15 gives the relationship between the maximum power outputs with the input frequencies when the exciting force amplitude fixed on 1360 N, and Figure 16 gives the relationship between the maximum power outputs with the force amplitude when the frequency of the excitation fixed on 6 Hz. Based on the Figure 15 and Figure 16, it can be obtained that the electrical energy which can be harvested by the proposed harvester is proportional to the frequency of external harmonic excitation and is proportional to the square of the force amplitude of the harmonic excitation. Therefore, the proposed piezoelectric energy harvester is a linear system, the output power increases with the external excitation level in the considered frequency and force.

#### **4. Conclusion**

Feasibility of a compression-based piezoelectric multilayer stack energy harvester as a promising alternative power for wireless sensor networks in civil structure health monitoring applications is investigated in this paper. Investigation of energy harvesting of such system for large force vibration existing in civil structure applications carried out theoretically and experimentally. Based on the linear theory of piezoelectricity, this paper presents the theoretical analysis of the piezoelectric multilayer stack harvester.



The theoretical analysis which has been verified with a series of experimental results can be used to synthetically analyze the behavior of vibration-to-electricity of the compression-type piezoelectric stack harvesting system. The experimental results show that the proposed piezoelectric stack harvester can generate up to 200 mW electrical power under harmonic excitation and it is sufficient for powering most normal wireless sensors. Additionally, based on the theoretical analysis and experimental results, the following conclusions can be acquired:

- (1) The electrical power scavenged by the proposed piezoelectric harvester depends not only on the harvester itself but also on the external electrical load. There is an optimal electrical load for a given exciting vibration, with which the electrical power harvested by the harvester reaches maximum value.
- (2) The optimal electrical load is inversely proportional to exciting frequency, and the value of the optimal electrical load does not affected by the force amplitude of excitation. Under the same input frequency, the optimal electrical load keeps in a constant value for different force amplitudes.
- (3) The proposed compression-based piezoelectric energy harvester is a linear system, the electrical energy which can be harvested by the proposed vibration harvester increases with the frequency and force amplitude of the harmonic excitation.

#### **Acknowledgements**

This work was supported by the National Science Foundation of China under Grand 51175265.

#### **References**

- [1] K. A. Cook-Chennault, N. Thambi, and A. M. Sastry, *Powering MEMS portable devices—a review of non-regenerative and regenerative power supply systems*

- with special emphasis on piezoelectric energy harvesting systems*, Smart Mater. Struct. 17 (2008), pp. 043001 (33pp).
- [2] C. O. Mathuna, T. O'Donnell, R. V. Martinez-Catala, J. Rohan, and B. O'Flynn, *Energy scavenging for long-term deployable wireless sensor networks*, Talanta 75 (2008), pp. 613-623.
- [3] C. B. Williams, and R. B. Yates, *Analysis of a micro-electric generator for Microsystems*, The 8<sup>th</sup> International Conference on Solid-State Sensors and Actuators, and Eurosensors IX. Stockholm, Swden, 25-29 June, 1995, pp. 369-372.
- [4] S. R. Anton, and H. A. Sodano, *A review of power harvesting using piezoelectric materials (2003-2006)*, Smart Mater. Struct. 16 (2007), pp. R1-R21.
- [5] A. Harb, *Energy harvesting: state-of-the-art*, Renew. Energ. 36 (2011), pp. 2641-2654.
- [6] H. Wu, L. Tang, Y. Yang, and C. K. Soh, *A novel two-degrees-of-freedom piezoelectric energy harvester*, J. Intell. Mater. Syst. Struct. 24 (2012), pp. 357-368.
- [7] N. Elvin, A. Elvin, and D. H. Choi, *A self-powered damage detection sensor*, J. Strain Anal. Eng. Des. 38 (2003), pp. 115-124.
- [8] F. M. Discenzo, D. Chung, and K. A. Loparo, *Pump condition monitoring using self-powered wireless sensors*, Sound and Vibration 40 (2006), pp. 12-15.
- [9] M. Lallart, D. Guyomar, Y. Jayet, L. Petit, E. Lefeuvre, T. Monnier, P. Guy, and C. Richard, *Synchronized switch harvesting applied to self-powered smart systems: piezoactive microgenerators for autonomous wireless receivers*, Sens. Actuators A 147 (2008), pp. 263-272.
- [10] S. H. Kim, J. H. Ahn, H. M. Chung, and H. W. Kang, *Analysis of piezoelectric effects on various loading conditions for energy harvesting in a bridge system*, Sensors and Actuators A 167 (2011), pp. 468-483.
- [11] S. Roundy, P. K. Wright, and J. Rabaey, *A study of low level vibrations as a power source for wireless sensor nodes*, Computer Communications 26 (2003), pp. 1131-1144.
- [12] L. Gu, *Low-frequency piezoelectric energy harvesting prototype suitable for the MEMS implementation*, Microelectron. J. 42 (2011), pp. 277-282.
- [13] P. D. Mitcheson, E. M. Yeatman, G. K. Rao, A. S. Holmes, and T. C. Green, *Energy harvesting from human and machine motion for wireless electronic devices*, Proceedings of the IEEE 96 (2008), pp. 1457-1486.
- [14] S. R. Platt, S. Farritor, and H. Haider, *On low-frequency electric power generation with PIEZOELECTRIC ceramics*, IEEE/ASME Trans. Mechatronics 10 (2005), pp. 240-252.
- [15] N. E. duToit, B. L. Wardle, and S. Kim, *Design considerations for MEMS-scale piezoelectric mechanical vibration energy harvesters*, Integrated Ferroelectrics 71 (2005), pp. 121-160.
- [16] N. G. Elvin, and A. A. Elvin, *A general equivalent circuit model for piezoelectric generators*, J. Intell. Mater. Syst. Struct. 20 (2008), pp. 3-9.

- [17] A. Erturk, and D.J. Inman, *Issues in mathematical modeling of piezoelectric energy harvesters*, Smart Mater. Struct. 17 (2008), pp. 065016 (14pp).
- [18] S. Roundy, E. S. Leland, J. Baker et al., *Improving power output for vibration-based energy scavengers*, IEEE Pervasive Computing 4 (2005), pp. 28-36.
- [19] O. Aldraihem and A. Baz, *Energy harvester with a dynamic magnifier*, J. Intell. Mater. Syst. Struct. 22 (2011), pp. 521-530.
- [20] L. H. Tang and Y. W. Yang, *A multiple-degree-of-freedom piezoelectric energy harvesting model*, J. Intell. Mater. Syst. Struct. 23 (2012), pp. 1631-1647.
- [17][21] H. Wu, L. H. Tang, P. V. Avvari, Y. W. Yang, and C. K. Soh, *Broadband energy harvesting using nonlinear 2-DOF configuration*, Proc. SPIE 8688, Active and Passive Smart Structures and Integrated Systems 2013, 86880B.
- [18][22] C. Keawboonchuay, and T. G. Engel, *Design, modelling, and implementation of a 30-kW piezoelectric pulse generator*, IEEE Trans. Plasma Sci. 30 (2002), pp. 679–686.
- [19][23] C. Keawboonchuay, and T.G. Engel, *Scaling relationships and maximum peak power generation in a piezoelectric pulse generator*, IEEE Trans. Plasma Sci. 32 (2004), pp. 1879–1885.
- [20][24] S. R. Platt, S. Farritor, and H. Haider, *The use of piezoelectric ceramics for electric power generation within orthopaedic implants*, IEEE/ASME Trans. Mechatronics 10 (2005), pp. 455–461.
- [25] J. Feenstra, J. Granstrom, and H. Sodano, *Energy harvesting through a backpack employing a mechanically amplified piezoelectric stack*, Mech. Syst. Signal Pr. 22 (2008), pp. 721–734.
- [21][26] INNOWATTECH LTE., *Energy harvesting*, International Patent (WO 2009/098676 A1).

Formatted: Font: Italic, English (U.S.)

Formatted: Font: Italic, English (U.S.)

Formatted: Font: Italic, English (U.S.)

Formatted: Font: Italic, English (U.S.)

Formatted: Font: Italic, English (U.S.)

Table 1. Characteristic properties of the piezoelectric stack

Figure 1. Construction of the piezoelectric stack

Figure 2. Longitudinal mode of the piezoelectric stack

Figure 3. 2DOF electromechanical model of the proposed harvester

Figure 4. Sketch of the test setup

Figure 5. Photo of the test setup

Figure 6. Spring stiffness static test from MTS machine

Figure 7. The applied force vs. output voltage under 20mm/2Hz motion

Figure 8. Output voltage under 680N/2Hz excitation

Figure 9. Output voltage vs. electrical loads under 680N/2Hz excitation

Figure 10. Output power vs. electrical loads under 680N/2Hz excitation

Figure 11. Output voltage comparison under different excitations with same frequency

Figure 12. Output voltage comparison under different excitations with same frequency

Figure 13. Output voltage comparison under different excitations with same force amplitude

Figure 14. Harvested power comparison under different excitations with same force amplitude

Figure 15. Maximum harvested power vs. exciting frequency

Figure 16. Maximum harvested power vs. exciting force amplitude

Table 1. Characteristic properties of the piezoelectric stack

Material properties	Value	Stack properties	Value
Material type	PZT-8	Diameter (mm)	20
Coupling factors $k_{33}$	0.68	Height $h_p$ (mm)	34
Piezoelectric constant $d_{33}$ (pC/N)	280	Single wafer thickness $t$ (mm)	0.85
Dielectric constants $\epsilon_{33}/\epsilon_0$	1000	Layer number	36
Young's modulus $YE_{33}$ ( $10^{10}$ N/m)	7.1	Mass $m_p$ (g)	87
Curie point ( $^{\circ}\text{C}$ )	320	Capacitance $C_p$ ( $\mu\text{F}$ )	0.12
Density ( $10^3$ kg/m $^3$ )	7.7	Natural frequency $\omega_n$ ( $10^9$ N/m)	1.1

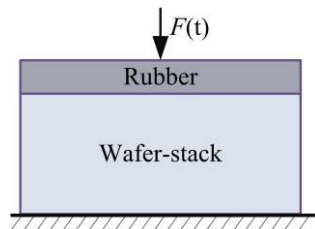


Figure 1. Construction of the piezoelectric stack

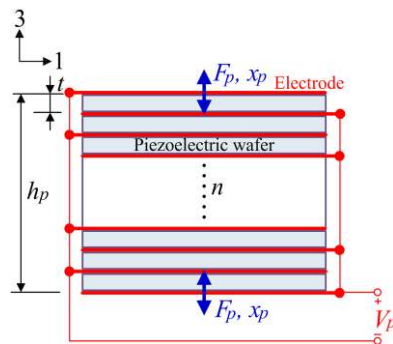


Figure 2. Longitudinal mode of the piezoelectric stack

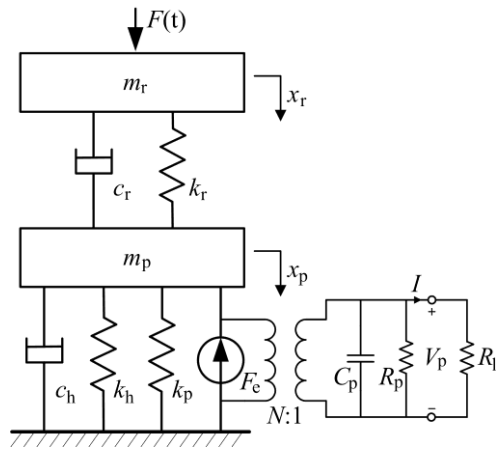


Figure 3. 2DOF electromechanical model of the proposed harvester

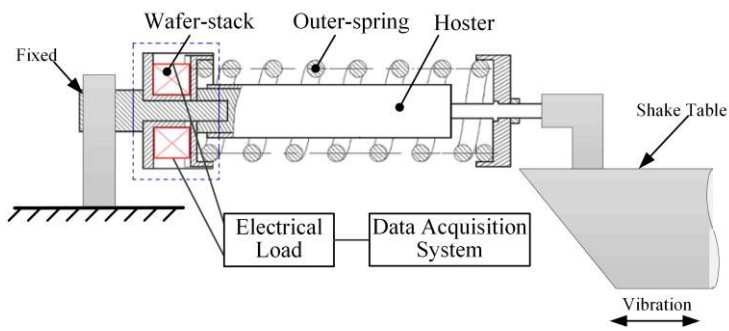


Figure 4. Sketch of the test setup

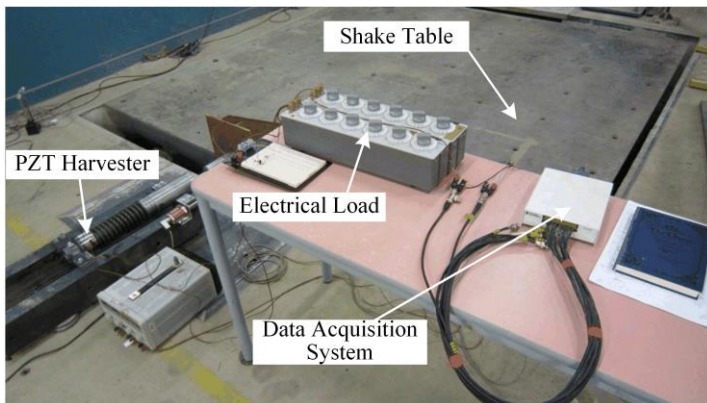


Figure 5. Photo of the test setup

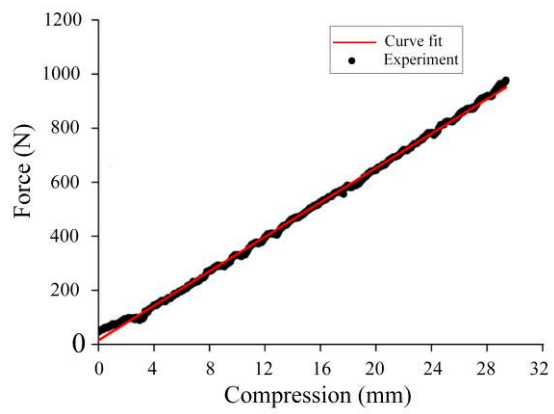


Figure 6. Spring stiffness static test from MTS machine

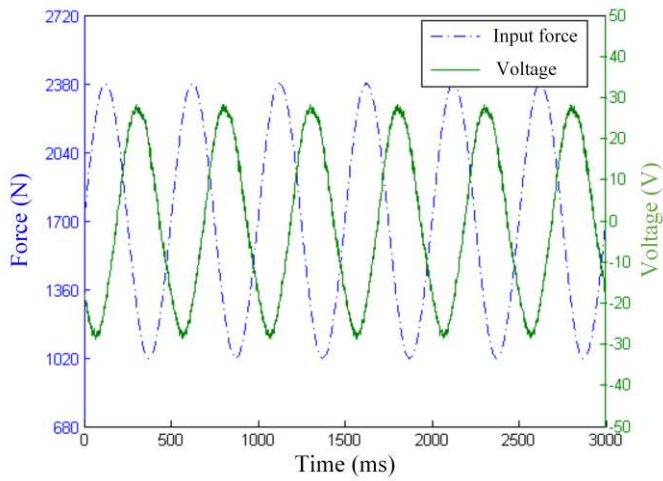


Figure 7. The applied force vs. output voltage under 20mm/2Hz motion

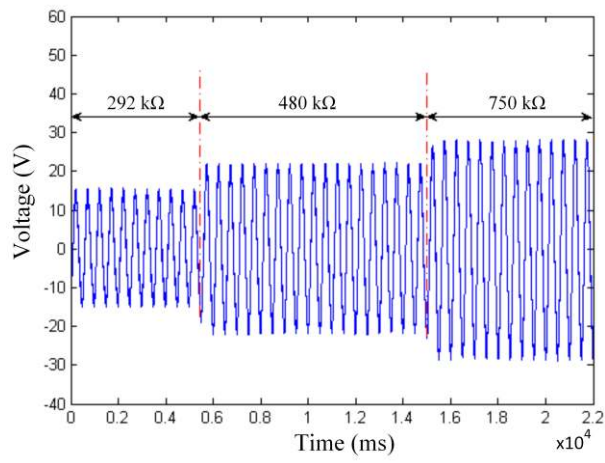


Figure 8. Output voltage under 680N/2Hz excitation

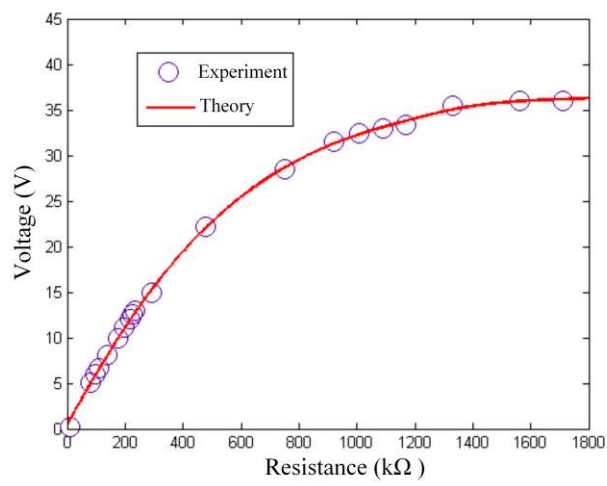


Figure 9. Output voltage vs. electrical loads under 680N/2Hz excitation



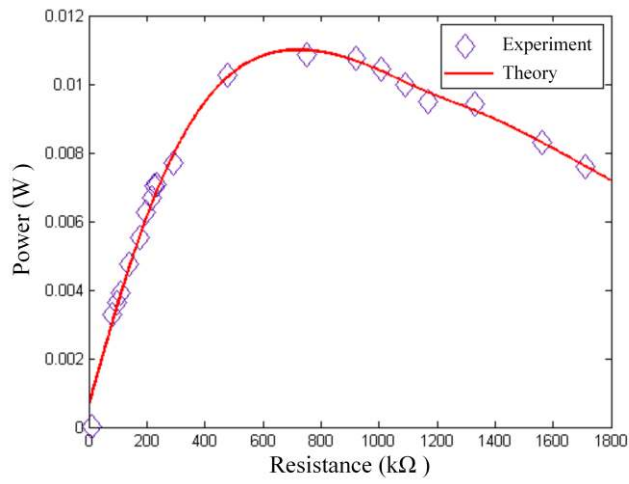


Figure 10. Output power vs. electrical loads under 680N/2Hz excitation

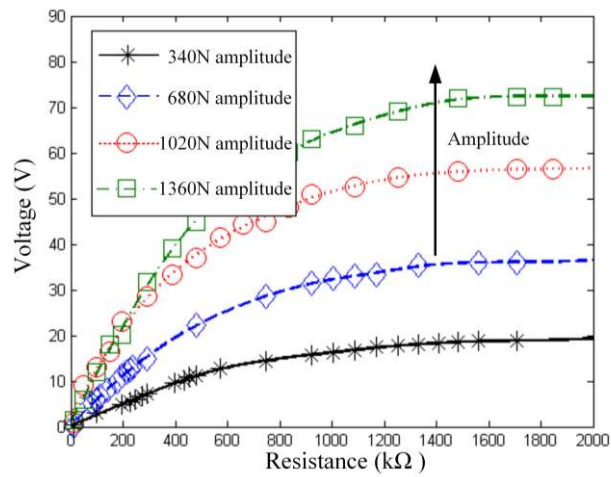


Figure 11. Output voltage comparison under different excitations with same frequency

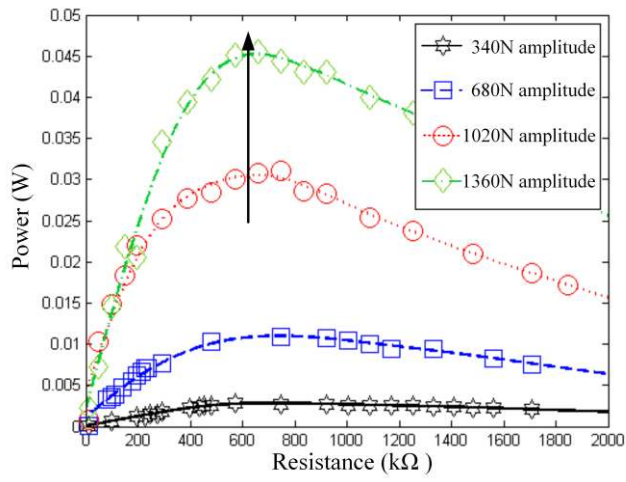


Figure 12. Harvested power comparison under different excitations with same frequency

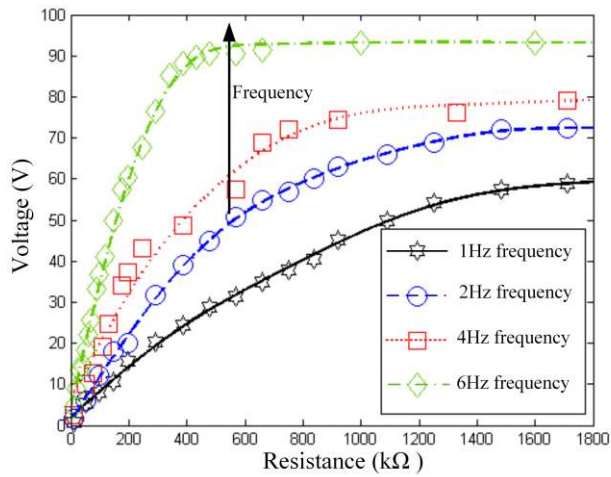


Figure 13. Output voltage comparison under different excitations with same force amplitude

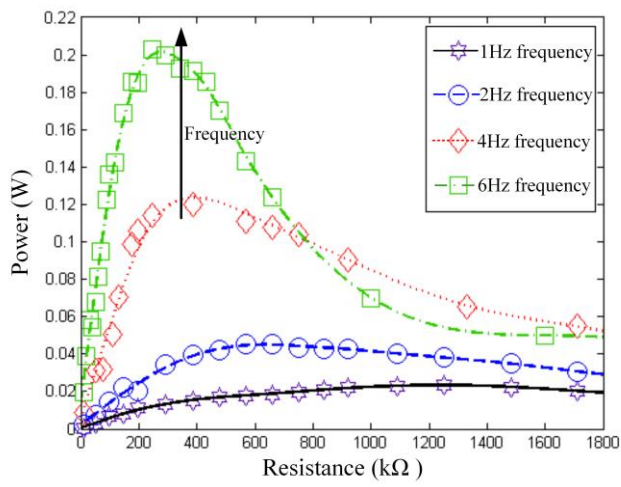


Figure 14. Harvested power comparison under different excitations with same force amplitude

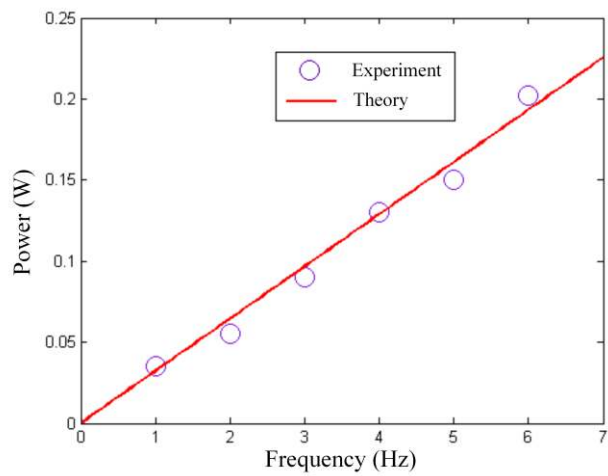


Figure 15. Maximum harvested power vs. exciting frequency

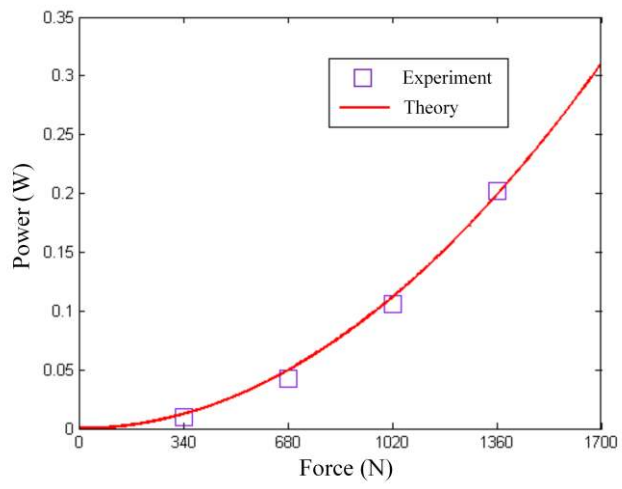


Figure 16. Maximum harvested power vs. exciting force amplitude